

**Abstract** Timo Noack github: Timtomtum141 edX acc:  
Timo<sub>6</sub>0

## 1 Introduction

I joined this workshop to obtain a broader understanding of silicon photonics. In frame of the course we obtained a fundamental understanding of silicon waveguides and different key components. For the practical tests we were allowed to design different structures which will be fabricated and analyzed afterwards. I concentrated on different Mach-Zehnder interferometers (MZI) as there are many key aspects of the course affecting the design. Furthermore, the design involves two waveguides with different lengths as calibration standards. I think this design will give me a good first insight in the silicon photonics thematics. The designs were designed in Klayout and simulatively varified by Ansys Lumerical. I hope to get an insight how well the simulated results match to the measurements of the structures.

## 2 Theory

### Waveguide Theory

All waveguides used in the design were strip waveguides with a width of 500 nm and a height of 220 nm. The excitations of the design are all defined for TE polarization. For this standard geometry we verifed the mode profiles in the waveguide section of the course by the finite-difference eigenmode solver of Lumerical MODE. The field distributions of the fundamental TE mode are plotted in Fig 1.

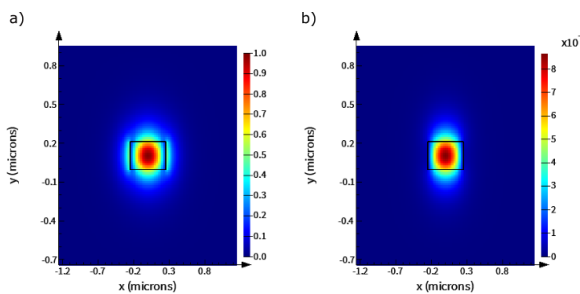


**Fig. 1** a) The x-component of the simulated electric field at lambda = 1550 nm. b) y-component of the H-field of the first TE mode

For the chosen geometry the simulations revealed a effective index of  $n_{\text{eff}} = 2.44$  and the group index

was  $n_g = 4.2$  with a TE polarization fraction of 0.98, indicating that the waveguide is effective single moded by excitation in TE polarization. This is important to minimize dispersive effects.

For the extraction of the effectice index and the group index for the fundamental mode a wavelength sweep between 1500 nm and 1600 nm was carried out (results see Fig 2).

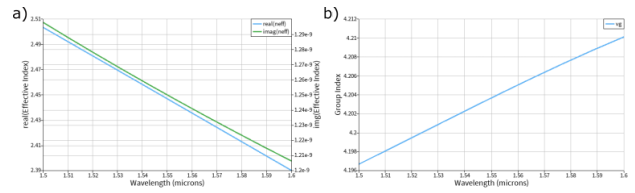


**Fig. 2** a) Effective index of the fundametal mode b) group index of the fundamental mode

Furthermore a compact model for the waveugide was derived by fitting the obtained values for the effective index by a second order polynomial function:

$$n_{\text{eff}}(\lambda) = n_1 + n_2(\lambda - \lambda_0) + n_3(\lambda - \lambda_0)^2$$

For the fit we obtained following parameters:

$$\begin{aligned} n_1 &= 2.446 \\ n_2 &= -1.133 \frac{1}{mm} \\ n_3 &= -0.041 \frac{1}{mm^2} \end{aligned}$$

3

4

## 5 Modelling and Simulation

For the design I generated different structures out of the above discussed waveguide system. The device of interest was here the MZI. For this purpose I designed three different designs, varying the length of the imbalance. In addition I designed two waveguides to determine both the transmission (and loss) of the waveguides as well as the wavelength dependent coupling efficiency of the grading couplers. The desing can be seen in Fig 3.

The two waveguides on the right side were included as reference measurements. The most important information we obtain by this strucuture is a measure of the coupling losses of the grating-couplers. These couplers show serious coupling losses with a strong wavelenght dependency. The characteristics of the grating couplers

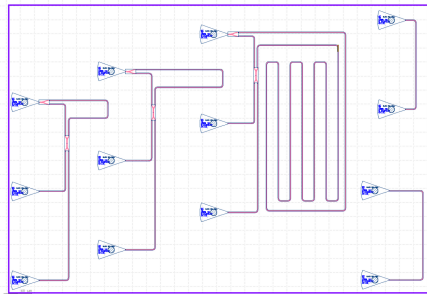


**Fig. 3** Final design for fabrication

can be also seen in the transfer functions of the MZIs. Thus, such a measurement allows us to subtract the grating-coupler influences of the MZI data.

Additionally, I want to obtain verification of waveguide losses. I expect slight differences due to the two different waveguide lengths. According to the simulation no big differences are expected. However, in the course we learned that the losses originate mainly due to scattering of the light at the roughness of the surface on the sides of the waveguide which is not taken into account at the simulations. Thus, I am curious if the difference in the transmission is visible at the end.

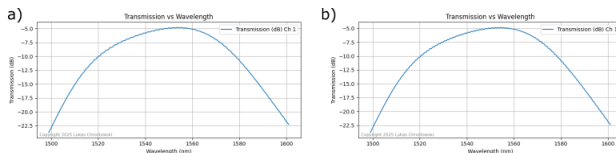


**Fig. 4** Transmission of a) the shorter and b) the longer waveguide

## 6 Mach-Zehnder interferometer

For the evalutaion of the MZI design three different geometries were chosen. The main difference in the three designs is the lenght of the imbalance. In this easy MZI design the imbalance is solely generate by a path length difference of the two input paths. The MZIs were designed in Klayout and simulatively checked by application of the SiEPIC-EBeam-PDK and the following simulation in Lumerical INTERCONNECT.

In an MZI two input signals are combined. The two input signals can overlay destructive or constructive or in between at the output regarding of the phase

and amplitude differences at the input. In the here investigated designs a single input signal is split 50/50 into two seperated paths. In case of a balanced MZI the transferfunction is then only defined by the propagation constant in the two splitted branches according to equation:

$$\frac{I_o}{I_i} = \frac{1}{2} (1 + \cos (\Delta\beta L))$$

where  $\Delta\beta$  corresponds to the difference in the propagation constant in both input arms. However, in unser design we intentionally implemented a length difference in both splitted arms while the waveguide width and heights in both arms was identical. For this scenario, the propagation constants in both arms are identical and the transferfunction is solely defined by the path length difference:

$$\frac{I_o}{I_i} = \frac{1}{2} (1 + \cos (\beta\Delta L))$$

By this equation we obtain the periodicity between fully destructive and fully constructive interference. This information can be also expressed in terms of the free spectral range (FSR) which specifies the spacing of two neighboring transmission peaks:

$$\text{FSR} = \frac{\lambda^2}{\Delta L n_g}$$

In my design I have chosen the length differences  $\Delta L = 118.6 \text{ mm}$ ,  $200 \text{ mm}$ ,  $2100 \text{ mm}$ . This corresponds to FSR values of  $\text{FSR} = 4.8 \text{ nm}$ ,  $2.9 \text{ nm}$ ,  $0.27 \text{ nm}$  for the lines closest to  $1.55 \mu\text{m}$ , respectively. Measurements the design will allow us to verify these values.

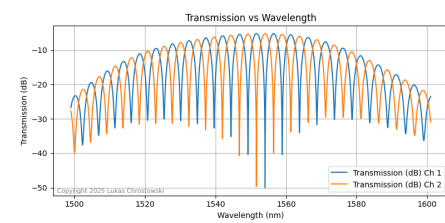


**Fig. 5** Transferfunction for the MZI with the shortest imbalance length of  $\Delta L = 118.6 \text{ mm}$

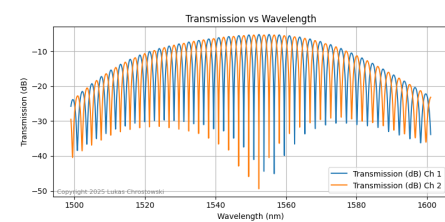


**Fig. 6** Transferfunction for the MZI with the intermediate imbalance length of  $\Delta L = 200 \text{ mm}$

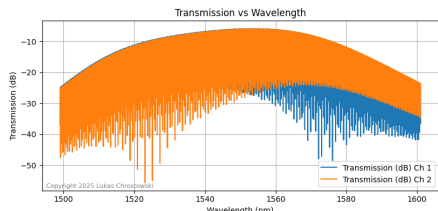


**Fig. 7** Transferfunction for the MZI with the longest imbalance length of  $\Delta L = 2100\text{ mm}$

## 7 Fabrication

Two chips were fabricated in this course. Either report on one dataset, or on both. Choose the text as appropriate.

### 7.1 Washington Nanofabrication Facility (WNF) silicon photonics process:

The devices were fabricated using 100 keV Electron Beam Lithography [[1]]. The fabrication used silicon-on-insulator wafer with 220 nm thick silicon on 3  $\mu\text{m}$  thick silicon dioxide. The substrates were 25 mm squares diced from 150 mm wafers. After a solvent rinse and hot-plate dehydration bake, hydrogen silsesquioxane resist (HSQ, Dow-Corning XP-1541-006) was spin-coated at 4000 rpm, then hotplate baked at 80 °C for 4 minutes. Electron beam lithography was performed using a JEOL JBX-6300FS system operated at 100 keV energy, 8 nA beam current, and 500  $\mu\text{m}$  exposure field size. The machine grid used for shape placement was 1 nm, while the beam stepping grid, the spacing between dwell points during the shape writing, was 6 nm. An exposure dose of 2800  $\mu\text{C}/\text{cm}^2$  was used. The resist was developed by immersion in 25% tetramethylammonium hydroxide for 4 minutes, followed by a flowing deionized water rinse for 60 s, an isopropanol rinse for 10 s, and then blown dry with nitrogen. The silicon was removed from unexposed areas using inductively coupled plasma etching in an Oxford Plasmalab System 100, with a chlorine gas flow of 20 sccm, pressure of 12 mT, ICP power of 800 W, bias power of 40 W, and a platen temperature of 20 °C, resulting in a bias voltage of 185 V. During etching, chips were mounted on a 100 mm silicon carrier wafer using perfluoropolyether vacuum oil.

## 7.2 Applied Nanotools, Inc. NanoSOI process:

The photonic devices were fabricated using the NanoSOI MPW fabrication process by Applied Nanotools Inc. (<http://www.appliednt.com/nanosoi>; Edmonton, Canada) which is based on direct-write 100 keV electron beam lithography technology. Silicon-on-insulator wafers of 200 mm diameter, 220 nm device thickness and 2  $\mu\text{m}$  buffer oxide thickness are used as the base material for the fabrication. The wafer was pre-diced into square substrates with dimensions of 25x25 mm, and lines were scribed into the substrate backsides to facilitate easy separation into smaller chips once fabrication was complete. After an initial wafer clean using piranha solution (3:1 H<sub>2</sub>SO<sub>4</sub>:H<sub>2</sub>O<sub>2</sub>) for 15 minutes and water/IPA rinse, hydrogen silsesquioxane (HSQ) resist was spin-coated onto the substrate and heated to evaporate the solvent. The photonic devices were patterned using a Raith EBPG 5000+ electron beam instrument using a raster step size of 5 nm. The exposure dosage of the design was corrected for proximity effects that result from the backscatter of electrons from exposure of nearby features. Shape writing order was optimized for efficient patterning and minimal beam drift. After the e-beam exposure and subsequent development with a tetramethylammonium sulfate (TMAH) solution, the devices were inspected optically for residues and/or defects. The chips were then mounted on a 4" handle wafer and underwent an anisotropic ICP-RIE etch process using chlorine after qualification of the etch rate. The resist was removed from the surface of the devices using a 10:1 buffer oxide wet etch, and the devices were inspected using a scanning electron microscope (SEM) to verify patterning and etch quality. A 2.2  $\mu\text{m}$  oxide cladding was deposited using a plasma-enhanced chemical vapour deposition (PECVD) process based on tetraethyl orthosilicate (TEOS) at 300°C. Reflectometry measurements were performed throughout the process to verify the device layer, buffer oxide and cladding thicknesses before delivery.

## 8 Experimental Data

To characterize the devices, a custom-built automated test setup [[2]] with automated control software written in Python was used (<http://siepic.ubc.ca/probestation>). An Agilent 81600B tunable laser was used as the input source and Agilent 81635A optical power sensors as the output detectors. The wavelength was swept from 1500 to 1600 nm in 10 pm steps. A polarization maintaining (PM) fibre was used to maintain

the polarization state of the light, to couple the TE polarization into the grating couplers [[3]]. A 90° rotation was used to inject light into the TM grating couplers [4]. A polarization maintaining fibre array was used to couple light in/out of the chip [www.plcconnections.com].

Plots of experimental data. The following figure was generated using a built-in Python interpreter!

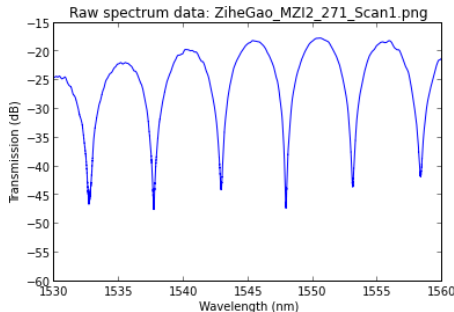


**Fig. 8** Measured transmission spectrum on a Mach-Zehnder Interferometer with a path length difference of x microns.

## 9 Analysis

Data analysis to extract waveguide group index, etc.

Comparison of experimental results with simulations.

## 10 Conclusion

The conclusion goes here.

## 11 Acknowledgements

\*\*(edit according to your use).\*\*

I/We acknowledge the edX UBCx Phot1x Silicon Photonics Design, Fabrication and Data Analysis course, which is supported by the Natural Sciences and Engineering Research Council of Canada (NSERC) Silicon Electronic-Photonic Integrated Circuits (SiEPIC) Program. The devices were fabricated by Richard Bojko at the University of Washington Washington Nanofabrication Facility, part of the National Science Foundation's National Nanotechnology Infrastructure Network (NNIN), and Cameron Horvath at Applied NanoTools, Inc. Enxiao Luan performed the measurements

at The University of British Columbia. We acknowledge Lumerical Solutions, Inc., Mathworks, Mentor Graphics, Python, and KLayout for the design software.

## References

1. Bojko RJ, Li J, He L, et al. (2011) Electron beam lithography writing strategies for low loss high confinement silicon optical waveguides. *Journal of Vacuum Science & Technology B: Microelectronics and Nanometer Structures* 29:06F309. <https://doi.org/10.1116/1.3653266>
2. Chrostowski L, Hochberg M Testing and packaging. In: *Silicon Photonics Design*. Cambridge University Press (CUP), pp 381–405
3. Wang Y, Wang X, Flueckiger J, et al. (2014) Focusing sub-wavelength grating couplers with low back reflections for rapid prototyping of silicon photonic circuits. *Opt Express* 22:20652. <https://doi.org/10.1364/oe.22.020652>